860469

Effect of Drop Breakup on Fuel Sprays

R. D. Reitz
and R. Diwakar
Fluid Mechanics Dept.
GM Research Laboratories
Warren, MI

ABSTRACT

Recently developed computer models are being applied to calculate complex interactions between sprays and gas motions. The three- dimensional KIVA code was modified to address drop breakup and was used to study fuel sprays. The results show that drop breakup influences spray penetration, vaporization and mixing in high pressure sprays. The spray drop size is the outcome of a competition between drop breakup and drop coalescence phenomena, and the atomization details at the injector are lost during these size rearrangements. Drop breakup dominates in hollow-cone sprays because coalescence is minimized by the expanding spray geometry. The results imply that it may be possible to use a simple injector and still control spray drop size and vaporization if the flow details are modified so as to enhance drop breakup and coalescence.

FUEL INJECTED ENGINES OFFER the potential for improved fuel economy and reduced fuel sensitivity. Progress towards these goals has been slow due to the complexity of the combustion and fuel injection processes. However, recent advances in experimental and computational techniques are providing new opportunities for progress. Multidimensional models are now available which can be used to study key processes and also to suggest means for their control. However, these models are still being developed and this requires validation by comparison with detailed and informative experiments.

Encouraging results have already been obtained for modeling single-phase flows in the absence of combustion [1].† The problem of modeling two-phase flow with fuel injection is addressed in this work. For this purpose, a recently developed multidimensional computer model, KIVA [2], was used to study unconfined, non-combusting, fuel sprays and the results were compared with experimental data [3].

One of the main difficulties in existing spray models is the specification of drop size at the injector, since the atomization process is poorly understood. Experimental analysis of atomization is difficult since the spray near the injector is optically dense and drop sizes cannot be measured, except near the edge of the spray [4]. However, drops at the spray edge may not represent drops formed from the atomization process within the spray.

Previous attempts to model sprays have used experimental correlations for initial

---

† Numbers in brackets designate references listed at the end of this paper.

0096-736X/87/9503-0218$02.50

drop size derived from edge measurements [5], and also from indirect measurements of the spray cone angle [6]. These modeling efforts indicate that the downstream spray drop size is not sensitive to the assumed initial drop size [6]. However, as will be seen in the present study, this is because drop coalescence phenomena have an important effect on the downstream sizes within those solid-cone sprays.

In hollow-cone sprays, coalescence is less important and therefore the downstream drop size could be expected to depend on the assumed initial drop size. The purpose of the present study was to assess the implications of inadequate knowledge of the initial drop size and to establish the importance of secondary atomization phenomena within the spray (due to drop breakup).

MODEL

The governing equations and the numerical solution method of the model are described by Amsden et al. [2] . An explicit numerical method is used with acoustic subcycling to solve the 3-dimensional gas conservation equations and a Lagrangian treatment is applied to the drops. Stochastic parcel injection is used to represent the spray drops for computational efficiency. In the present computations, the gas phase mass, momentum and energy equations were supplemented by a k-ε turbulence model which accounts for turbulence diffusion [5,7]. The computational drops exchange mass, momentum and energy with the gas using the dense spray correlations of O'Rourke and Bracco [8]. Droplet dispersion due to turbulence is modeled using a random walk method [9]. The walk durations are related to the drop residence time within an eddy or to the eddy lifetime, whichever is smaller. Drop collision and coalescence are also included in the model [8].

The injected drop size for hollow-cone spray computations was specified using an atomization model that is derived from a stability analysis of liquid sheets [10]. This analysis gives

$$SMR = 8.4\ C^{-3/2}\ \xi\ (\rho_2/\rho_1)^{1/2} \qquad (1)$$

where SMR is the Sauter Mean Radius,

ξ is the sheet breakup length,

$$\xi/\delta = C\ \{(\frac{\rho_1}{\rho_2})(\frac{\sigma}{\rho_2 U^2 \delta})(\frac{h}{\delta})\frac{1}{\tan\theta}\}^{1/3}$$

and ρ_1 and ρ_2 are the liquid and gas densities, respectively, and σ is the surface tension. θ is the cone angle, δ is the poppet seat diameter, h is the sheet thickness at the nozzle exit, and U is the injection velocity. A χ^2-distribution was assumed for the injected drops. The atomization model used for solid-cone spray computations was that of Reitz and Bracco [11].

Drop breakup was modeled starting from the correlations given in the review by Nicholls [12] where two breakup regimes are identified: bag breakup when

$$We=\rho_2 w^2 r/\sigma > 6.0 \quad ; \qquad (2)$$

(We is the Weber number) (the factor 6.0 was taken in Eq. (2) as a representative value. Literature values vary between 3.6 and 8.4) and stripping breakup when

$$We/\sqrt{Re} > 0.5 \qquad (3)$$

where the Reynolds number $Re=2wr/\nu$, ν is the kinematic viscosity and r is the drop radius.

The lifetimes of unstable drops are

$$t_1 = D_1 \left[\frac{\rho_1 r^3}{\sigma}\right]^{1/2} \qquad (4)$$

$$t_2 = D_2 \frac{r}{w} (\rho_1/\rho_2)^{1/2} , \qquad (5)$$

for the bag and stripping modes, respectively. The bag breakup time, Eq. (4), is assumed to be proportional to the drop natural frequency. In Eq. (5), w is the relative velocity between the drop and the gas and the constant D_2 is of order unity [12].

Unfortunately there is little information available about the drop size distribution which results from the breakup of a parent drop. As a first attempt to account for drop breakup, the following method and assumptions were adopted. The stability criteria, Eqs. (2) and (3), were checked for each drop parcel at each timestep. If either of the two criteria continued to be met for a time equal to the corresponding time in Eqs. (4) or (5), then a new drop size for the parcel was specified using either Eq. (2) or Eq. (3) (depending on which breakup criterion was exceeded) as an equality (i.e. it was assumed that the new drops were marginally stable). Actually, it was observed in the present computations that bag-type breakup seldom occurs.

Care was taken to ensure mass, momentum and energy conservation during the above 'breakup' procedure (see Appendix A).

RESULTS

HOLLOW-CONE SPRAY - The top panels in Figs. 1a, 1b and 1c show high speed movie frames (0.222 ms between frames) of a hollow-cone, Indolene spray from an oscillating poppet injector, taken from Shearer and Groff [3]. In this experiment the liquid was injected into quiescent room temperature nitrogen at 550 kPa. To model their bomb experiments, a cylindrical computational domain (diameter and height equal to 40 mm) with free-slip boundary conditions was used. The grid had 19x16x24 cells in the diametral, azimuthal and axial directions, respectively, as shown in Fig. 2. (Other numerical experiments with a finer mesh confirmed that the results are grid-independent). The numerical timestep was fixed (2.5 μs) and about 2000 spray parcels were in the computation at the

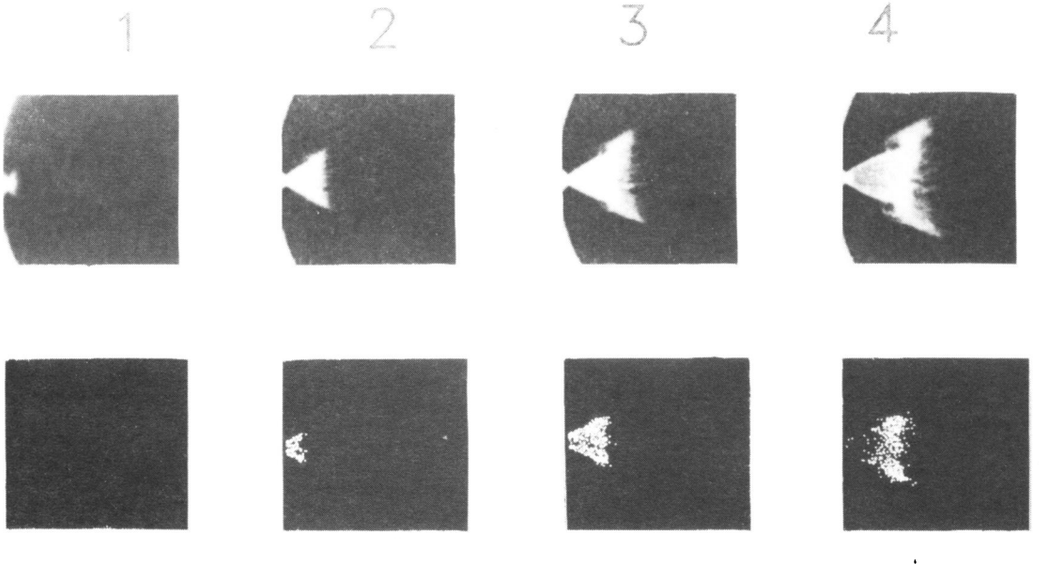

FIGURE 1a. Comparison of computed 3-dimensional spray parcel locations with spray photographs of Ref. [3]. Frames 1-4. 0.222 ms between frames. Drop breakup is included in the model.

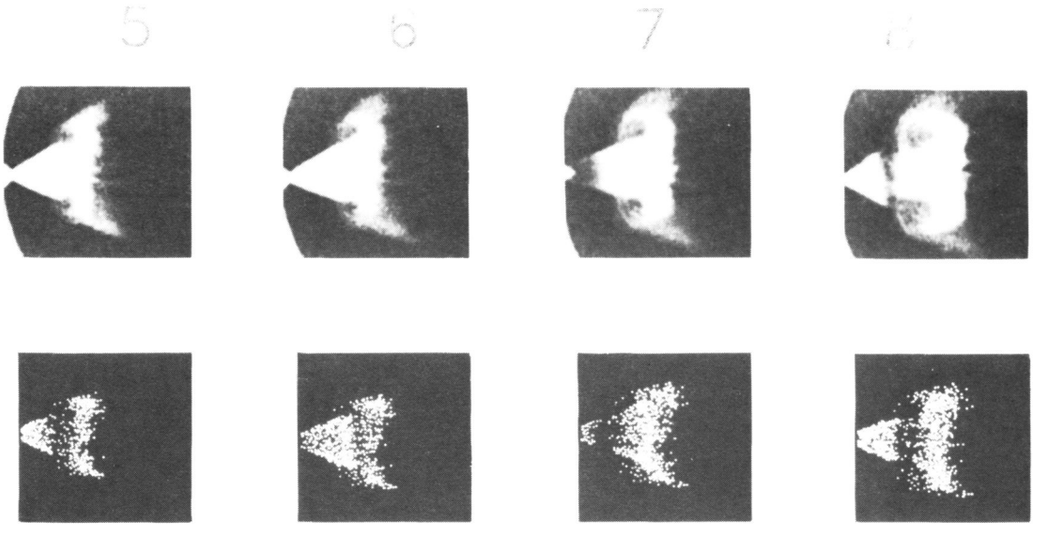

FIGURE 1b. Comparison of computed 3-dimensional spray parcel locations with spray photographs of Ref. [3]. Frames 5-8. 0.222 ms between frames. Drop breakup is included in the model.

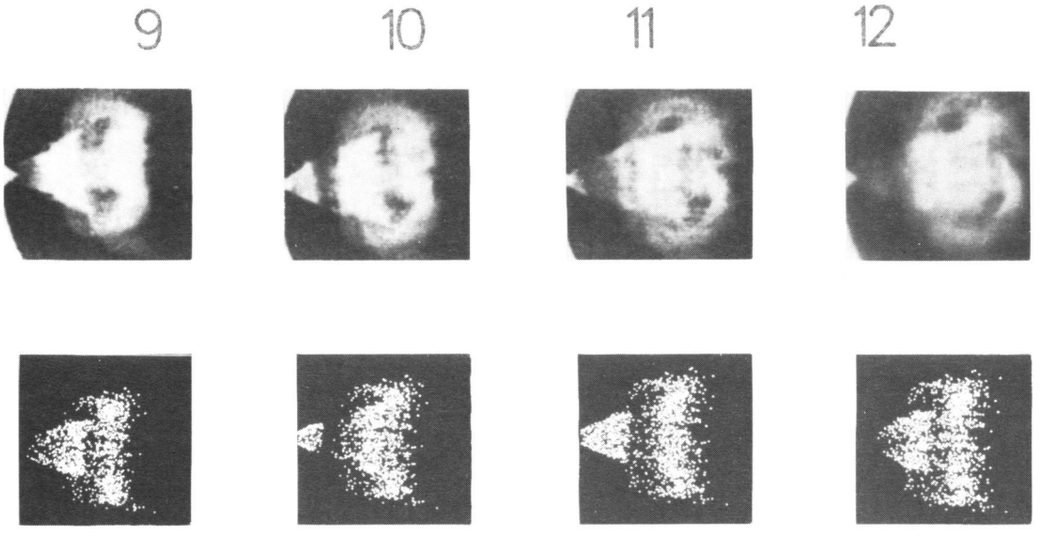

FIGURE 1c. Comparison of computed 3-dimensional spray parcel locations with spray photographs of Ref. [3]. Frames 9-12. 0.222 ms between frames. Drop breakup is included in the model.

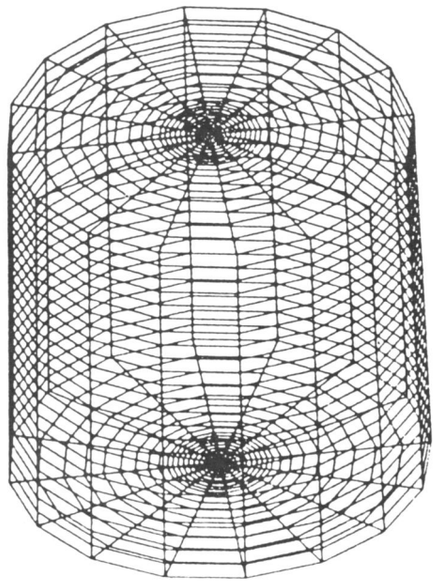

FIGURE 2. Computational grid used in the calculations.

end of each injection. To save computer time, axisymmetry was assumed for some computations and for those cases the 2-dimensional version of KIVA was used.

The experimental spray cone angle for the spray of Fig. 1 was 60 degrees, the nozzle seat diameter 2.4 mm, and the flow rate 0.0165 mL/injection with four pulses, each of duration about 0.58 ms. The measured liquid injection pressure is shown in Fig. 3. The pressure data was used to estimate the number and the duration of the spray pulses. These and other pressure measurements [13] also indicated that the injection velocity could be approximated as a constant throughout the injection. Thus the computational injection velocity was set equal to the experimental spray tip velocity measured from the movie pictures early in the injection. (The measured tip velocity was 60 m/s for the injection of Fig. 1 [3]).

A sine-squared variation of poppet lift (or liquid sheet thickness, h) with time was assumed and the maximum lift was found from the measured fuel flow and injection velocity. When this postulated sheet thickness variation with time is used in Eq. (1) with C=20, the injected spray drop size varies as is shown by the dotted line in Fig. 3.

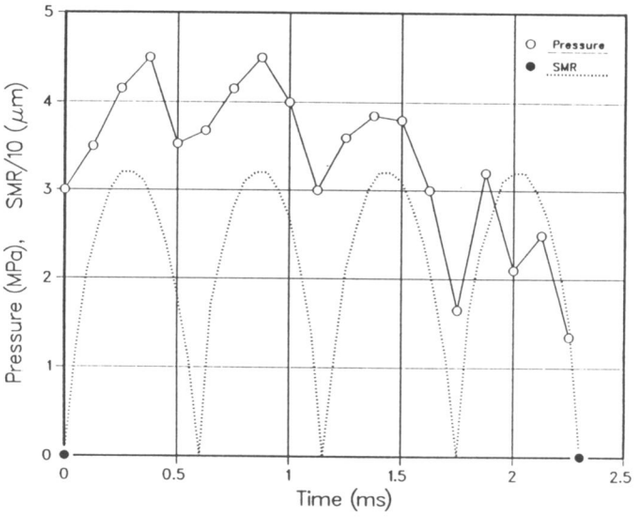

FIGURE 3. Measured liquid injection pressure versus time [3] showing four spray pulses. The dashed line shows initial Sauter Mean Radius of the injected drops using Eq. (1) with C=20.

Spray tip penetration measured from the pictures of Fig. 1 early in the injection is shown in Fig. 4 (dotted line). The figure also shows predicted spray tip penetration without including drop breakup in the computations. The four different symbols correspond to different values of the atomization constant C in Eq. (3) (12, 20, 147 and 432 giving SMR=42, 32, 12 and 7 μm for the injected drop size at maximum poppet lift, respectively). It is seen that large C values (small initial drop sizes) are required in order to match the experiment.

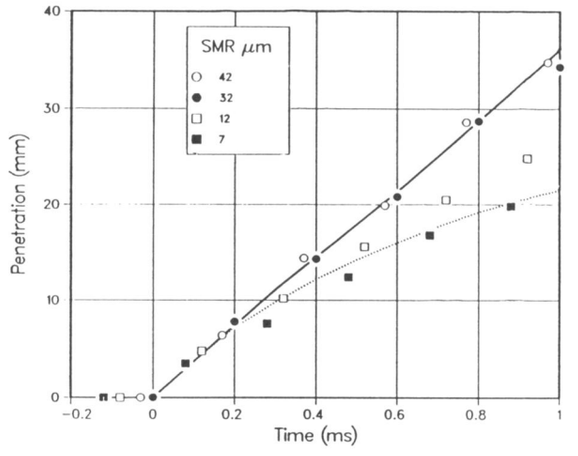

FIGURE 4. Pulsed hollow-cone spray penetration versus time. Dashed line - experiment (see also Fig. 1). Solid line - constant velocity jet. Symbols - computations without drop breakup each using a different initial Sauter Mean Radius.

In Fig. 4 the beginning of injection is shifted to earlier times as the injected drop size decreases. This was necessary to match the experimental penetration. It is difficult to assess the implications of this shift in the origin because the flow at the beginning of injection is unsteady and it could not be resolved at the frame rate of the experiments. However, the computed penetration was found to be insensitive to further reductions in the initial SMR beyond 7 μm. This is because the number of injected drops increases with decreasing initial drop size (for the same fuel flow) and drop collision and coalescence become more and more significant as the drop number increases. The above behavior compensates for the smaller initial drop size.

The minute initial drop size required to match the experiments is not consistent with other sheet breakup data [10]. These studies would place the maximum initial SMR between 30 and 40 μm. This large discrepancy prompted consideration of drop breakup.

The computed tip penetrations shown in Fig. 5 (symbols) include drop breakup. The corresponding experiments (lines) cover a broad range of gas pressures (factor of 15) [3]. The computations used C=20 in Eq. (1) and D_1=1 and D_2=0.5 in Eqs. (4) and (5) to give best agreement with the 550 kPa results. It is seen that the calculations also predict the experimental tip penetration adequately over the entire tested range of gas pressures with the same set of constants.

Other calculations made with different values of C in Eq. (1) showed that the tip penetration and the downstream drop size are not sensitive to the atomization drop size when drop breakup is included.

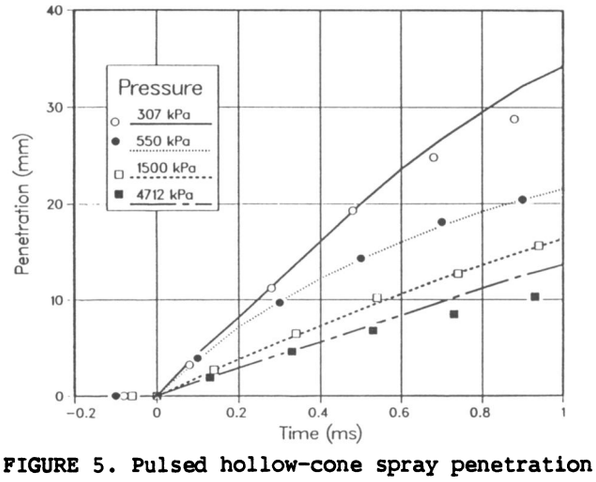

FIGURE 5. Pulsed hollow-cone spray penetration versus time. Lines - experiments of Shearer and Groff [3]. Symbols - computed penetration at different gas pressures with drop breakup.

Details of the computed spray structure are presented in the lower panels of Figs. 1a, 1b and 1c for comparison with the 550 kPa gas pressure experiments. The 3-D results show the spray parcels along a line-of-sight through the spray (i.e. all spray parcels are plotted). The computed spray shapes agree well with the experiment throughout the injection.

The vortex seen at the spray tip in the photographs is also evident in the computations. This flow structure is present in the

gas velocity vector plot of Fig. 6 which shows the flow field at t=2.1 ms after the start of injection, i.e. frame 11, Fig. 1c. The head vortex is produced by the spray pulsations and it has the effect of increasing the radial extent of spray penetration and mixing.

The head vortex consists of small entrained drops as can be seen by referring to Fig. 7b. Here the numbers summarize the computed spray drop size for selected drop parcels from the parcel plot of Fig. 7a. (There are too many parcels in Fig. 7a for all to be included in Fig. 7b). The recirculating vortex region consists of '1' parcels (drop size 0-10 μm) while the leading edge of the head has '2' (10-20 μm) and '3' (20-30 μm) parcels.

Figure 7b also highlights drop coalescence and breakup phenomena. The injected drops are seen as '3' at the top of the figure. This follows from the assumed atomization drop size (20-30 μm) shown in Fig. 3. The locally high drop number density in the region of the injector favors drop collision and coalescence producing a few shortlived '7' parcels (60-70 μm) which subsequently break up as the spray penetrates the gas.

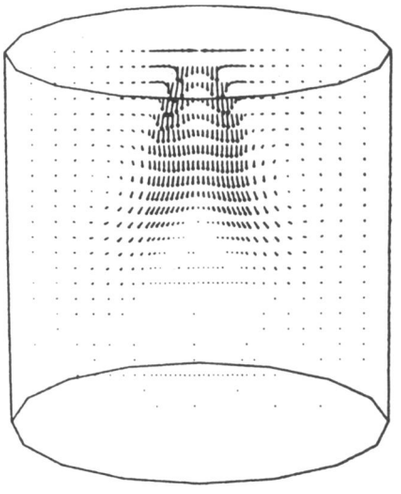

FIGURE 6. Computed gas velocity vectors in a symmetry plane at 2.1 ms after beginning of injection (i.e. frame 11 Fig. 1) showing head vortex details. Maximum axial, radial and azimuthal velocities are 31.3, 12.4 and 2.1 m/s, respectively.

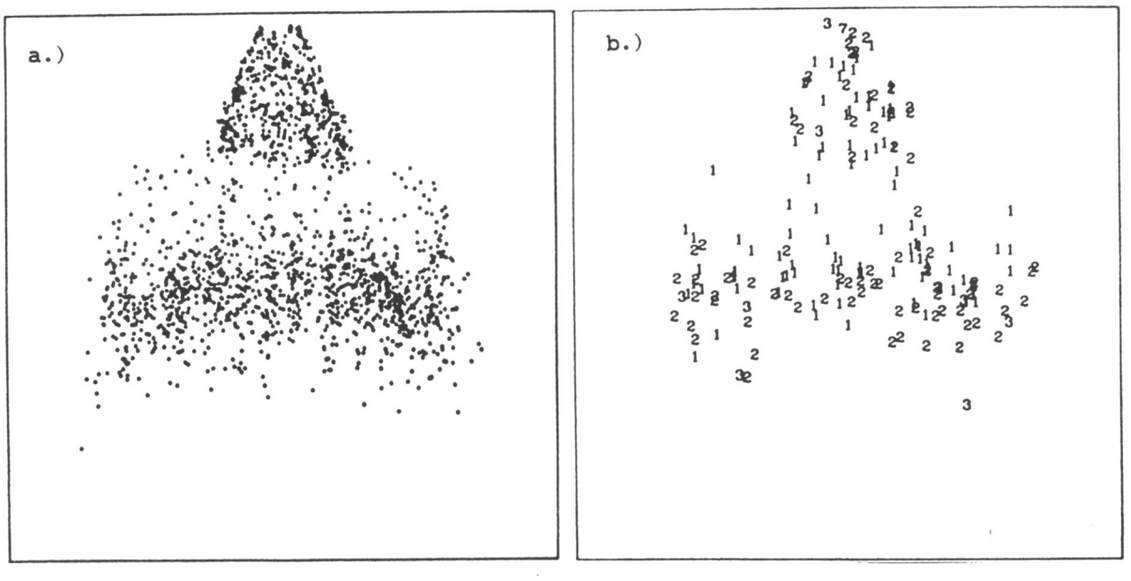

FIGURE 7. Computed spray parcel plots at 2.1 ms after the beginning of injection (i.e. frame 11, Fig. 1) showing a.) drop parcel locations b.) parcel drop radius. '1' = 0-10 μm, '2' = 10-20 μm etc.

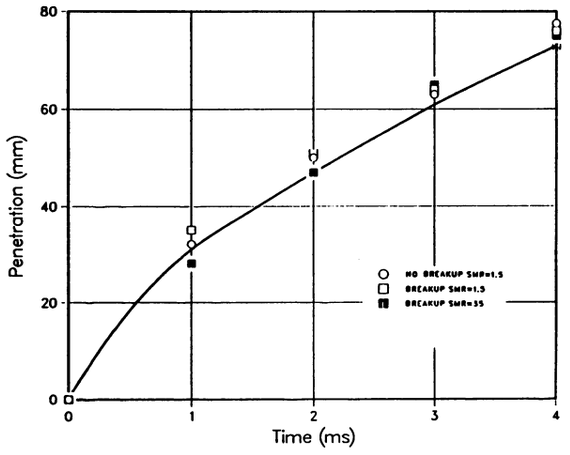

FIGURE 8. Steady solid-cone spray penetration versus time. Solid line - experiment of Hiroyasu and Kadota [14]. Symbols - computations without (circles) and with drop breakup (squares), initial SMR = 1.5 μm. Solid squares - drop breakup with initial SMR = 35 μm.

SOLID-CONE SPRAY - The open symbols in Fig. 8 show computed spray penetrations for a solid-cone spray with (squares) and without drop breakup (circles). The solid line shows the corresponding experiment of Hiroyasu and Kadota [14]: diesel oil injection (injection pressure 9.9 MPa) into compressed nitrogen at 3 MPa from a single hole nozzle with diameter 0.3mm. The computations were made with constant turbulence diffusivity (3.9×10^{-4} m²/s) and initial SMR=1.5 μm and the conditions were chosen to allow comparison with the results of Kuo and Bracco [6] (the circles reproduce their case number 2). The breakup constants D_1 and D_2 were as for the hollow-cone spray calculations above.

Figure 8 shows that the computed tip penetration is the same with and without drop breakup. The solid squares show the effect of arbitrarily increasing the initial SMR to 35 μm with drop breakup also included in the model. The computed penetration is also seen to be insensitive to the atomization drop size. Insensitivity of spray penetration to atomization parameters without drop breakup was also noted by O'Rourke and Bracco [8] for solid-cone sprays. This is because details of the initial atomization process are overshadowed by drop coalesence, which determines the drop sizes downstream of the injector.

Figure 9 shows the corresponding computed drop size variation with distance from the injector for the spray of Fig. 8 (SMR is averaged over the spray cross-section at each axial station). The symbols are defined as in Fig. 8. The scatter is due to the statistical nature of the numerical solution technique and the lines are least square fits of the data. It is seen that smaller downstream drops are found when drop breakup is accounted for. Moreover the downstream drop size is not sensitive to the atomization drop size.

Coalescences are more numerous in solid-cone sprays than in hollow-cone sprays since the drops are closely packed and thus have high collision frequencies, particularly close to the injector. The downstream drop size is evidently determined by a competition between the coalescences (which decrease with increas-

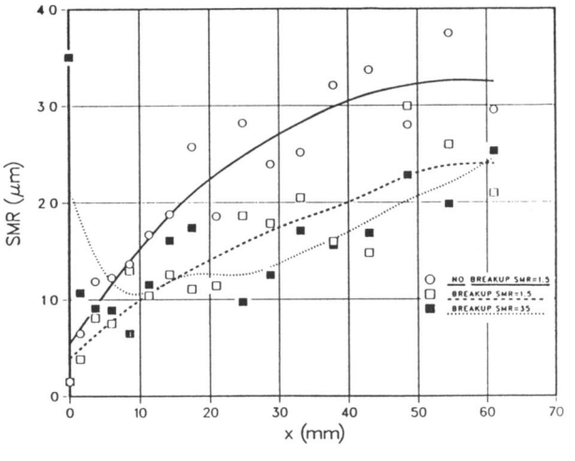

FIGURE 9. Computed drop size variation with distance from the injector for solid-cone spray. Symbols - computations without (circles) and with drop breakup (squares), initial SMR = 1.5 μm. Solid squares - drop breakup with initial SMR = 35 μm. Lines - least square fits of the data.

ing distance from the nozzle due to the expansion of the spray) and the breakups (which also decrease due to the reduced relative velocity between the drops and the entrained gas).

Interestingly, the computed downstream drop size with breakup shown in Fig. 9 is closer to the experimental value (SMR=24.5 [14]) than the case without breakup. But, as pointed out by Kuo and Bracco [6], drop sizes also depend on the injection schedule (the present computations assumed steady injection). However, the results show that drop breakup does influence the spray drop size, even in diesel-type sprays.

CONCLUSIONS

The results indicate that secondary atomization phenomena within the spray (drop breakup and coalescence) determine the drop size in high pressure sprays of interest to engine applications. Since vaporization rates depend on drop size, this implies that drop breakup/coalescence also influences the fuel vapor distribution and mixing.

It may be possible to control the distribution of fuel in practical devices by exploiting the competition between drop breakup and drop coalescence. This may be accomplished even with a relatively simple injector, since it is not necessary to control the drop size at the injector (spray drop size is determined by drop breakup/coalescence effects). The atomizer only serves to generate relative velocity between the liquid and the gas and this enhances the drop breakup. The injector also controls flow direction, or the spray geometry, and drop collision/coalescence rates can be influenced by the resulting drop spacing.

The details of the gas flow field have an important effect on the spray. Hence it should also be possible to influence the spray drop size, for example, by altering the details of the gas motion. In fact, many practical combustion chambers are designed to generate strong gas flows. This is known to have a significant effect on the spray and its combustion.

SUMMARY

- Drop breakup influences spray penetration, vaporization and mixing.
- Spray drop size is controlled by a dynamic balance between drop coalescences and drop breakups.
- Details of the initial atomization process are lost during the size rearrangements which occur within the spray.
- Drop breakup has a dominant effect on the spray drop size in hollow-cone sprays since drop coalescence is minimized by the expanding spray geometry.
- The downstream drop size in solid-cone sprays is influenced by both drop coalescence and breakup. A balance is reached as coalescences decrease (due to the expansion of the spray) and as breakup ceases (due to the reduced relative velocity between the drops and the entrained gas).

ACKNOWLEDGMENTS

The authors thank Roger Krieger and Bruce Peters for their helpful comments.

REFERENCES

1. C. Arcoumanis and J. H. Whitelaw, "Fluid Mechanics of Internal Combustion Engines: A Review," International Symposium on Flows in Internal Combustion Engines - III, Eds. T. Uzkan, W.G. Tiederman, J.M. Novak, ASME FED-Vol. 28, New York, 1985, pp. 1-17.

2. A. A. Amsden, J. D. Ramshaw, P. J. O'Rourke and J. K. Dukowicz, "KIVA: A Computer

Program for Two- and Three-Dimensional Fluid Flows with Chemical Reactions and Fuel Sprays," Los Alamos Report No. LA-10245-MS, February 1985.

3. A. J. Shearer and E. G. Groff, "Injection System Effects on Oscillating-Poppet-Injector Sprays," Proceedings of the ASME Diesel and Gas Engine Power Division Conference, Ed. A.A. Zagotta, New York, 1984, pp. 33-42.

4. K.-J. Wu, Atomizing Round Jets, Ph.D Thesis, Princeton University, 1983.

5. L. Martinelli, F. V. Bracco and R. D. Reitz, "Comparisons of Computed and Measured Dense Spray Jets," Progress in Astronautics and Aeronautics, Ed. M. Summerfield, Vol. 95, 1984, pp. 484-512.

6. T.-W. Kuo and F. V. Bracco, "Computations of Drop Sizes in Pulsating Sprays and of Liquid Core Length in Vaporizing Sprays," SAE paper No. 820133.

7. S. H. El Tahry, "k-ϵ Equations for Compressible Reciprocating Engine Flows," J. Energy, Vol. 7 , 1983, pp. 345-353.

8. P. J. O'Rourke and F. V. Bracco "Modeling of Drop Interactions in Thick Sprays and Comparison with Experiments," Institution of Mechanical Engineers, Pub. ISBN 0 85298 4693, 1980, pp. 101-116.

9. J. K. Dukowicz, "A Particle-Fluid Numerical Method for Liquid Sprays," J. Comp. Phys., Vol. 35, 1980, pp. 229-253.

10. N. Dombrowski and P. C. Hooper, "The Effect of Ambient Density on Drop Formation in Sprays," Chem. Eng. Sci., Vol. 17, 1962, pp. 291-305.

11. R. D. Reitz and F. V. Bracco, "Mechanism of Atomization of a Liquid jet," Phys. Fluids, Vol. 25, 1982, pp. 1730-1742.

12. J. Nicholls, "Stream and Droplet Breakup by Shock Waves," NASA SP-194, Eds. D.T. Harrje and F.H. Reardon, 1972, pp.126-128.

13. E. G. Groff and A. J. Shearer, Private Communication, General Motors Research Laboratories, Warren, Michigan, 1985.

14. H. Hiroyasu and T. Kadota, "Fuel Droplet Size Distribution in Diesel Combustion Chamber", SAE Paper 740715.

APPENDIX A

Mass, Momentum and Energy Conservation During Drop Breakup

Liquid mass at breakup was conserved by adjusting the number of drops in the parcel according to

$$n_f r_f^3 = n_i r_i^3 \qquad \text{(A1)}$$

where n is the number of drops and the subscripts f and i denote conditions after and before breakup, respectively. The drop surface energy increases at breakup. The energy equation is

$$m\,(\underline{u}.\underline{u})/2 + \sigma\pi r^2 n = \text{constant} \qquad \text{(A2)}$$

where $m=4\pi\rho_l r^3 n/3$ is the total parcel mass and $\underline{u}$ is the drop velocity vector. To conserve energy we reduced each of the drop's three velocity components by the factor δV where

$$\delta V = 1 - \left(\frac{r_i}{r_f} - 1\right) \frac{\sigma}{\rho_l r_i} \frac{3}{4\,\underline{u}.\underline{u}_i} \qquad \text{(A3)}$$

Equation (A3) is a linearized form of Eq. (A2). For consistency the momentum lost by the drops during this procedure, $m(\underline{u}_f - \underline{u}_i)$, was added to the gas momentum.

Actually these momentum and energy corrections proved to be small in our sprays. We include them in the model only for completeness.